Dentomaxillofacial Radiology (2018) 47, 20170361

birpublications.org/dmfr

RESEARCH ARTICLE

Evaluation and reduction of magnetic resonance imaging artefacts induced by distinct plates for osseous fixation: an in vitro study @ 3 T

[1,2]Carsten Rendenbach, [3]Max Schoellchen, [3]Julie Bueschel, [4]Tobias Gauer, [5]Jan Sedlacik, [5]Daniel Kutzner, [6]Pekka K Vallittu, [1]Max Heiland, [3]Ralf Smeets, [5]Jens Fiehler and [5]Susanne Siemonsen

[1]Department of Oral and Maxillofacial Surgery, Charité – Universitaetsmedizin Berlin, Corporate member of Freie Universität Berlin, Humboldt-Universität zu Berlin, and Berlin Institute of Health, Berlin, Germany; [2]Berlin Institute of Health (BIH), Berlin, Germany; [3]Department of Oral and Maxillofacial Surgery, University Medical Center Hamburg-Eppendorf, Hamburg, Germany; [4]Department of Radiotherapy and Radiation Oncology, University Medical Center Hamburg-Eppendorf, Hamburg, Germany; [5]Department of Diagnostic and Interventional Neuroradiology, University Medical Center Hamburg-Eppendorf, Hamburg, Germany; [6]Department of Biomaterials Science, Institute of Dentistry, University of Turku, and City of Turku, Welfare Division, Turku, Finland

Objectives: To analyze MRI artefacts induced at 3 T by bioresorbable, titanium (TI) and glass fibre reinforced composite (GFRC) plates for osseous reconstruction.
Methods: Fixation plates including bioresorbable polymers (Inion CPS, Inion Oy, Tampere, Finland; Rapidsorb, DePuy Synthes, Umkirch, Germany; Resorb X, Gebrueder KLS Martin GmbH, Tuttlingen, Germany), GFRC (Skulle Implants Oy, Turku, Finland) and TI plates of varying thickness and design (DePuy Synthes, Umkirch, Germany) were embedded in agarose gel and a 3 T MRI was performed using a standard protocol for head and neck imaging including T_1W and T_2W sequences. Additionally, different artefact reduction techniques (slice encoding for metal artefact reduction & ultrashort echo time) were used and their impact on the extent of artefacts evaluated for each material.
Results: All TI plates induced significantly more artefacts than resorbable plates in T_1W and T_2W sequences. GFRCs induced the least artefacts in both sequences. The total extent of artefacts increased with plate thickness and height. Plate thickness had no influence on the percentage of overestimation in all three dimensions. TI-induced artefacts were significantly reduced by both artefact reduction techniques.
Conclusions: Polylactide, GFRC and magnesium plates produce less susceptibility artefacts in MRI compared to TI, while the dimensions of TI plates directly influence artefact extension. Slice encoding for metal artefact reduction and ultrashort echo time significantly reduce metal artefacts at the expense of scan time or image resolution.
Dentomaxillofacial Radiology (2018) **47**, 20170361. doi: 10.1259/dmfr.20170361

Cite this article as: Rendenbach C, Schoellchen M, Bueschel J, Gauer T, Sedlacik J, Kutzner D, et al. Evaluation and reduction of magnetic resonance imaging artefacts induced by distinct plates for osseous fixation: an in vitro study @ 3 T. *Dentomaxillofac Radiol* 2018; **47**: 20170361.

Keywords: susceptibility artefacts; titanium; magnesium; glass fibre reinforced composites; resorbable polymers

Correspondence to: Dr Carsten Rendenbach, E-mail: carsten.rendenbach@charite.de

Received 29 September 2017; revised 23 March 2018; accepted 27 April 2018

Introduction

Osteosynthesis with plates and screws is commonly performed at the maxillofacial skeleton in trauma and reconstructive surgery. This particularly applies for the fixation of osseous free flaps for primary or secondary reconstruction after jaw resection due to osteonecrosis or malignoma.[1–6] As a standard feature, fixation of free flaps at the recipient site is performed with different titanium (TI) systems, basically combining screws with 1.0 mini- or 2.0–2.8 mm locking plates. Recently computer-assisted design/computer-assisted manufacturing (CAD/CAM) plates, which are virtually planned and milled to perfectly adapt to the transplant and recipient site, became increasingly popular for mandible reconstruction.[7]

As a standard feature in tumour follow-up programs after surgical and adjuvant therapy, MRI is regularly performed within the first 5 years after primary therapy.[8,9] If a plate removal is not performed, the persistent implants induce significant susceptibility artefacts in MRI.[10–12] These are caused by the presence of metallic materials and their higher susceptibility compared with surrounding tissues, which induces inhomogeneities in the magnetic field.[12–14] As a consequence, the quality and significance of the radiographic evaluation is reduced. Potentially, recurrent cancer and complications associated with implants, *e.g.* screw loosening or signs of inflammation, can easily be overseen or, briefly, are invisible to the reviewers.

Besides patient compliance, the extent of artefact induction depends on the implant's or plate's size, configuration, material and positioning itself, the MR field strength (1.5 *vs* 3 T), MR protocol and sequence parameters.[15] Accordingly, artefact reduction may be achieved via either the use of alternative fixation systems based on materials with less potential to induce susceptibility artefacts or by changing one or more parameters of MRI itself.

Regarding alternative materials like polylactic acids (PL),[16,17] magnesium (MG) and glass fibre reinforced composites (GFRCs) with higher fatigue strength are promising.[18–26] While GFRC is not bioresorbable and has to be fixed with screws of a different material, PL based copolymers degrade enzymatically via acidic hydrolysis and MG undergoes corrosion into magnesium hydroxide and hydrogen gas.[27]

However, to date, there is a certain lack of biomechanical, clinical and radiographic studies investigating advantages and disadvantages of these materials for mandible reconstruction.

For the reduction of artefacts induced by dental restorations, plates and screws, various metal artefact reduction techniques have recently been described. Conventional techniques include the use of 1.5 T instead of 3 T scanners by increasing the receiver bandwidth or matrix size, decreasing slice thickness, switching frequency and phase encoding direction and the usage of fat saturation with short TI inversion recovery (STIR) or Dixon sequences or subtraction images plus the use of fast spin echo sequences instead of gradient echo sequences.[15] Accordingly T_1 weighted (T_1W) and intermediate weighted sequences with shorter echo times (TEs) regularly induce less artefacts than T_2 weighted (T_2W) sequences with longer TE. In this regard, the ultrashort TE (UTE) sequence is an even more sophisticated metal artefact reduction sequence. UTE sequences use a different readout strategy delivering TEs far below 0.05 ms and by that reducing fast T_2 signal dephasing of tissues with very short T_2 relaxation times. Another promising approach to reduce artefacts is slice encoding for metal artefacts (SEMAC), *which* is used in combination with view angle tilting (VAT).[28–31] For maxillofacial TI systems, however, the impact of advanced metal artefact reduction sequences has not been evaluated to date. Further, there is a lack of knowledge regarding the extent and proportional increase of artefacts induced by varying thickness, design and material of fixation plates in MRI.

The aim of the current study was to compare the extent of susceptibility artefacts caused by fixation plates of varying material, thickness and design and the individual impact of SEMAC or UTE techniques to reduce artefacts at 3 T MRI *in vitro*. We hypothesized that, in descending order, artefacts by MG, GFRC and polylactide would be less pronounced than in TI and that the design and thickness of the plates has a relevant impact on artefact induction. We further hypothesized, that the potential of artefact reduction by UTE and SEMAC protocols would differ depending on the thickness and design of the plate.

Methods and materials

Plates

Susceptibility artefacts of bioabsorbable polymers [poly-L-lactide (PLLA), poly-D-L-lactide (PDLLA) or MG] and non-degradable GFRC and TI fixation plates were analyzed. In the TI group, conventional miniplates and locking plates of varying thickness were compared to a CAD/CAM locking plate. Table 1 provides an overview of the specimen used in the current study.

Embedding

All plates were positioned in the centre of a plastic container with the help of a resorbable suture (monocryl, 5–0) that was fixed to the container according to Figure 1a. Hereafter, the plates were embedded in 3% gelatin, with at least 3 cm of gel surrounding the probes in each direction. To avoid air/gelatin boundaries in the vicinity of the plates, the remaining space in containers was filled with sodium chloride (0.9%).

Table 1 Detailed manufacturer information on the specimen used in the study.

	Material	*Type of plate*	*Length (mm)*	*Height (mm)*	*Thickness (mm)*	*Manufacturer*
1	Titaniuma	*MatrixMANDIBLE* mini	41.0	4.5	1.0	Synthes[b]
2	Titanium[a]	*MatrixMANDIBLE* locking	48.0	7.0	2.0	Synthes[b]
3	Titanium[%a]	*ProPlan CMF* individual	40.0	8.0	2.0	Synthes[b]/Materialise[c]
4	Titanium[a]	*MatrixMANDIBLE* locking	48.0	8.0	2.8	Synthes[b]
5	Magnesium	Prototype	24.0	4.5	1.0	Meotec[d]
6	PLLA[g],PGA[h], PDLLA[i],TMC[j]	*CPS 2.5*	46.5	7.5	2.5	Inion[e]
7	PDLLA[i]	*RapidSorb*	42.0	7.5	1.2	Synthes[b]
8	PLLA[g]/PDLLA[i]	*Resorb X*	42.0	6.5	1.2	KLS Martin[f]
9	GFRC[j]	*Skulle* Individual	48.0	12.5	1.0	Skulle Implants Corporation[6]

GFRC, glass fibrereinforced composite; PDLLA, poly-D-L-lactide; PLLA, poly-L-lactide.
[a]Pure titanium.
[b]DePuy Synthes, Umkirch Germany: Ti-6Al-4V.
[c]Materialise GmbH, Leuven Belgium + DePuy Synthes, Umkirch, Germany.
[d]Meotec GmbH & Co. KG, Aachen, Germany.
[e]Inion Ltd., Tampere, Finland.
[f]KLS Martin Group, Tuttlingen, Germany.
[g]Poly-L-lactide acid.
[h]Poly-glycolic acid.
[i]Poly D-L-lactide acid.
[j]Tricalcium phosphate.
[k]Glass fibre reinforced composite: S glass with nominal composition of SiO_2 62%, Al_2O_3 26%, MgO 10%, B_2O_3 1%, Na_2O 0.5%, Fe_2O_3 0.2%. Glass fibre loading in dimethacrylate matrix: ca. 60 vol%.

Imaging

The embedded samples were scanned on a 3 T MR scanner (Skyra, Siemens Healthcare GmbH, Erlangen, Germany). The plates were positioned along their longitudinal axis within the magnetic field in order to simulate plate orientation at the mandible body (Figure 1b). The imaging protocol consisted of a T_2 weighted [three-dimensional (3D-T_2W)] space sequence [TE = 139 ms, repetition time (TR) = 2500 ms, slice thickness = 1 mm, 0.94 × 0.94 mm voxel size, matrix 192 × 192, field of view (FOV) 180] and a T_1 weighted (3D-T_1W) volumetric interpolated brain examination (VIBE) technique (TE = 2.46 ms, TR = 5.8 ms, slice thickness = 0.5 mm, 0.5 × 0.5mm voxel size, matrix 384 × 384, FOV 192) using a 32-channel head coil. To evaluate artefact reduction techniques, the following sequences were acquired:

T_2W STIR with SEMAC in axial, coronal and sagittal orientation [TE = 40 ms, TR = 7500 ms, inversion time (TI) = 200 ms, flip angle = 140°, slice thickness = 3 mm, 0.4 x 0.4 mm voxel size, matrix 192 × 192, FOV 160], T2w STIR (SEMAC_off) in axial, coronal and sagittal orientation [TE = 37 ms, TR = 7500 ms, TI = 200 ms, flip angle = 140°, slice thickness = 3 mm, 0.4 × 0.4 mm voxel size, matrix 192 × 192, FOV 160], 3D isotropic T_1W ultrashort TE (UTE) in transversal orientation (TE = 0.06 ms, TR = 7.91 ms, flip angle = 15°, slice thickness = 0.8 mm, 0.8 × 0.8 mm voxel size, matrix 256 × 256, FOV 200) and a T_1W volumetric interpolated brain examination

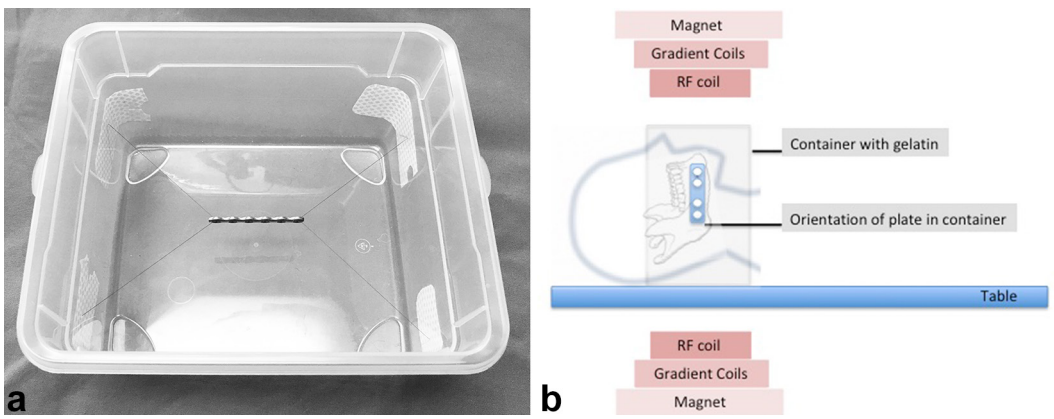

Figure 1 Exemplaric illustration of plate positioning in a plastic container (a) and plate/container positioning in the magnetic field (b) RF, radiofrequency.

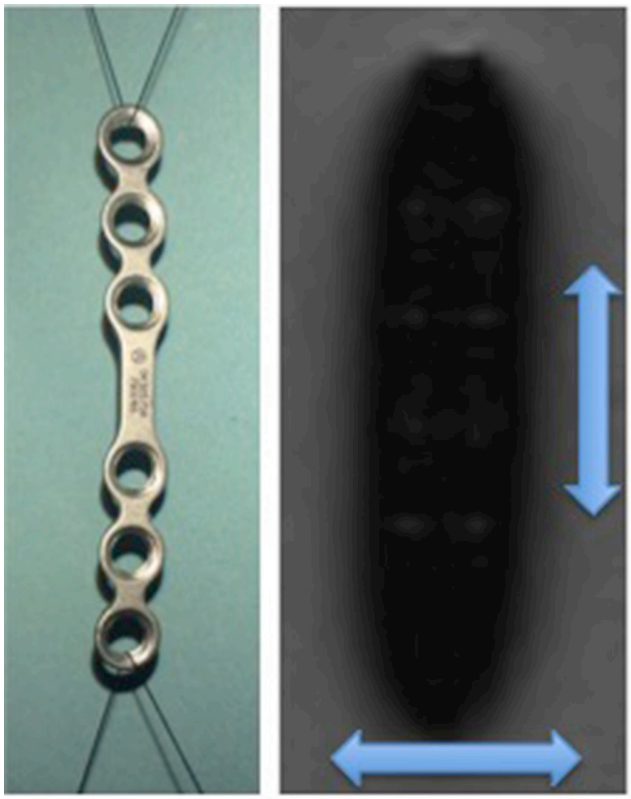

Figure 2 Exemplaric illustration of plate fixation in containers (left) and illustration of measurement of absolute artefact dimensions by two independent investigators (right).

technique (UTE_longTE) in axial orientation (TE = 1.23 ms, TR = 7.91 ms, flip angle = 15°, slice thickness = 0.8 mm, 0.8 × 0.8 mm voxel size, matrix 256 × 256, FOV 200).

Since SEMAC is only available as two-dimensional sequence, it was acquired in coronal, sagittal and transversal orientation in order to evaluate a potential dependence on acquisition orientation and the extent of artefact reduction.

It is technically not possible to use exactly the same sequence parameters for UTE and SEMAC as for the original T_1W and T_2W sequences, which could cause bias when directly comparing the artefact extent in both techniques. Applying artefact reduction techniques significantly increases the scan time. Therefore, the image resolution was reduced in both UTE and SEMAC, to obtain images with acceptable acquisition times. Therefore, additional analogous sequences applying the same parameters as for UTE and SEMAC but without artefact reduction technique were acquired (UTE_long TE and SEMAC_off) to ensure optimal comparability. Both, SEMAC and UTE were only used for TI and MG plates.

MRI data evaluation

Two researchers (CR and SS) independently measured the plates length, thickness and width in millimetres as indicated by signal voids on T_1W and T_2W images (Figure 2). Identical window width and level were applied using open-source OsiriX software.

For 3D sequences (3D-T_1W, 3D-T_2W), measurements were conducted on axial, coronal and sagittal reformatted images. For two-dimensional images (SEMAC, SEMAC-off, UTE, UTE-longTE), measurements were performed for all acquired planes.

Mean values of Reviewers 1 and 2 were calculated for each measurement and used for all further analyses.

Statistical analysis

All statistical analyses were performed using the software R (v. 3.2.0). The accuracy of size determination in MRI scans and corresponding ratios were calculated for T_1W and T_2W sequences for each material to assess the extent of artefacts produced by each fixation material and compare these between sequence techniques. The percentage of size overestimation was calculated as the size measured on MR images (corresponding to signal void), divided by the actual size of the plates (manufacturer's data, Table 1). The extent of artefacts with/without artefact reduction techniques was compared using paired *t*-test.

Results

Accuracy of size

All plates presented with a hypointense signal on T_1W and T_2W scans. Absolute and relative overestimation of size in 3D-T_1W and 3D-T_2W images are displayed in Figure 3 for each implant.

Overall the absolute and relative overestimation was significantly higher in T_2W than in T_1W images for all plates ($p < 0.01$).

Overall, TI plates showed higher absolute and relative size overestimation than polylactide and MG plates.

When comparing cumulative measurements of absolute overestimation of all dimensions for each implant, Synthes 2.8 (TI) and Synthes PSI (TI) showed the most pronounced artefact extent in 3DT_1W and 3DT_2W images, while Inion CPS (PL) and GFRC (PL) presented with the least extent of artefacts (Figure 3). Of all TI plates, the Synthes 1.0 (TI) presented with the least artefact extent. The amount of absolute overestimation was significantly associated with absolute plate thickness ($p < 0.001$, cor = 0.579) but not with plate length and height.

Artefact reduction techniques

The artefact reduction effect of UTE and SEMAC, *i.e.* the reduction of absolute overestimation is displayed in Figures 4 and 5.

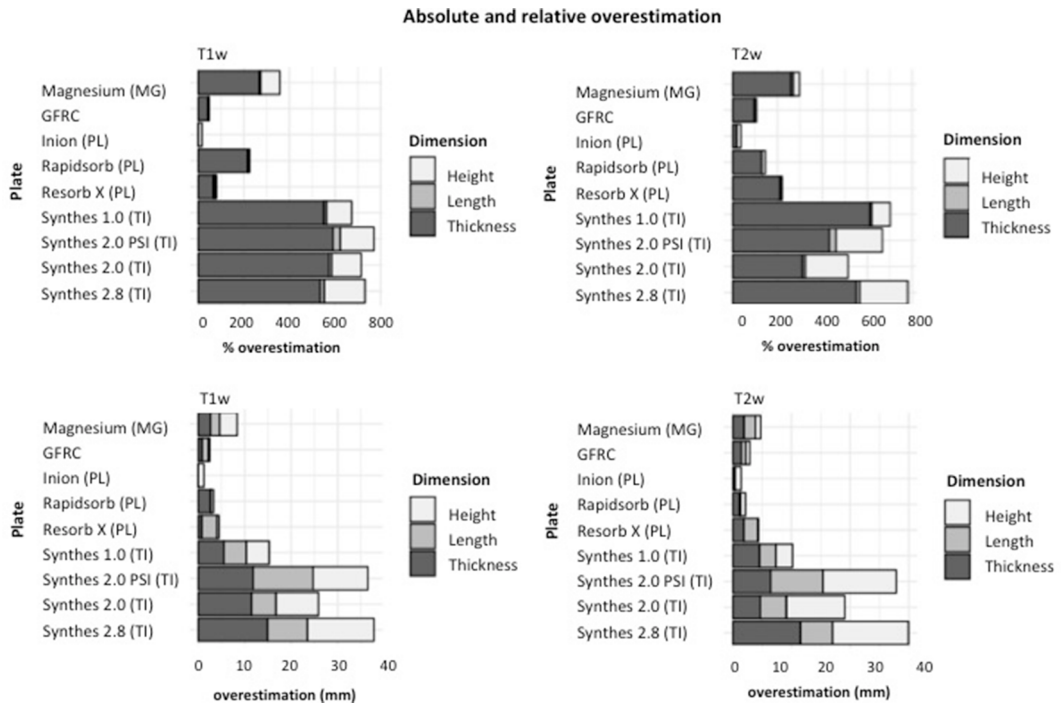

Figure 3 Absolute and relative overestimation in three dimensions in *T*1W and *T*2W of different fixation plates. GFRC, glassfibrereinforced composite; MG, magnesium; PL, polylactic acid; TI, titanium.

UTE

Overall, the absolute amount of implant size overestimation was significantly ($p < 0.001$) lower when using UTE [mean ± standard deviation (SD) ; 23.15 ± 18.34] in comparison to UTE_longTE scans (mean ± SD; 27.11 ± 17.84). Mean absolute artefact reduction by UTE was significantly higher ($p < 0.05$) for measurements in height (7.19 ± 3.95 mm) compared to implant length (2.20 ± 0.81 mm) and thickness (2.48 ± 1.15 mm).

When comparing different plates, the absolute amount of artefact reduction using UTE was lowest for Synthes 1.0 (TI) with a mean of 1.64 ± 0.98 mm, highest for Synthes 2.8 (TI) with 6.67 ± 5.93 mm. For all other TI plates, artefact reductions were comparable with the MG implant (Figure 4).

For SEMAC, the absolute overall amount of implant size overestimation was significantly ($p < 0.001$) lower when using artefact reduction technique (mean ± SD; 22.587 ± 17.35726) in comparison to SEMAC_off scans (mean ± SD; 28.286 ± 19.46587), (Figure 5).

For SEMAC, mean absolute artefact reduction was significantly higher ($p < 0.05$) for measurements in length (7.10 ± 4.10 mm) compared to implant height (5.07 ± 3.69 mm) and thickness (4.92 ± 4.73 mm).

Variances in the amount of artefact reduction were significantly ($p < 0.05$) higher for SEMAC than for UTE techniques for length and thickness.

When comparing different plates, the absolute amount of artefact reduction using SEMAC was lowest for Synthes 1.0 (TI) with a mean of 1.22 ± 0.73 mm, followed by MG with a mean of 3.67 ± 2.71, while mean values for the absolute amount of artefact reduction were highest but comparable for all other TI implants Synthes 2.8 (TI) with 8.62 ± 5.93 mm, Synthes 2.0 (TI) with 6.68 ± 2.96 mm and Synthes PSI (TI) with 8.31 ± 4.16 mm (Figure 5). Finally, Figure 6 provides an overview on each plate and used sequence in the study.

Discussion

Metal artefacts limit image quality in radiologic diagnostics and restaging of head and neck cancer patients. Impairment of image quality through fixation materials depending on the imaging modality used should be taken into consideration to achieve highest quality in diagnostics of primary or recurrent cancer. This may be achieved by using alternative (non-) metallic materials, including MG, polylactide and GFRCs as the base for patient specific solutions and as an alternative to TI. When TI use is inevitable, *e.g.* for biomechanical reasons, a reduction of the extent of the induced artefacts should be aimed for. In this regard, special scan protocols including UTE and SEMAC may help to reduce the amount of artefact pronunciation. This may still increase diagnostic image quality, although the use of these protocols limit sequence parameters and thus reduce image resolution. Further, the reduction of material dimensions thickness and height may help to improve image quality and diagnostic value.

In the present *in vitro* study, MG, polylactide and GFRC plates produced less artefacts than TI plates

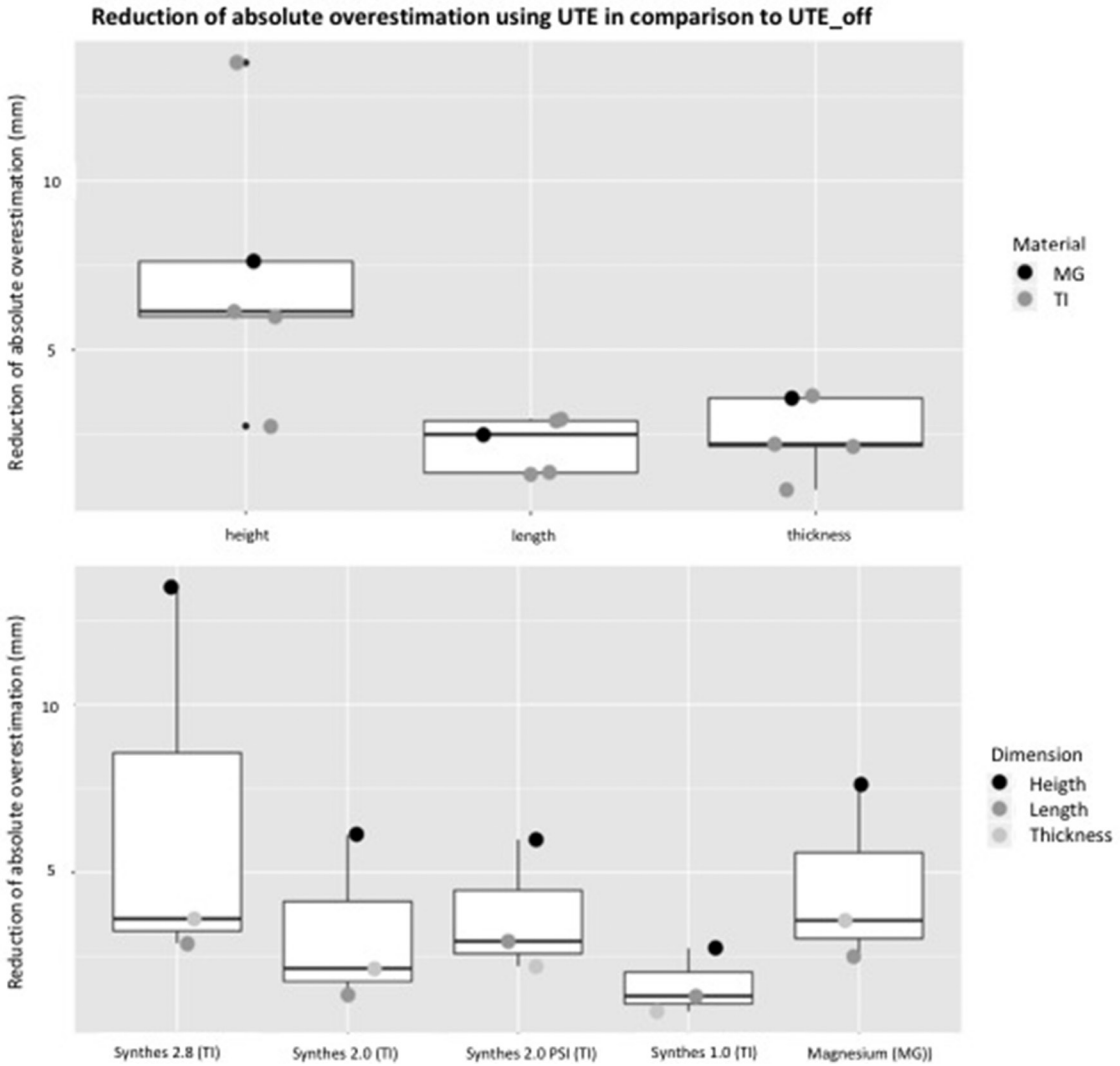

Figure 4 Reduction of absolute artefact overestimation for titanium and magnesium plates using UTE in comparison to UTE_longTE. UTE, ultrashort echo time.

of varying thickness and design when imaged with 3.0 T MRI, while artefacts on T_1W images were more pronounced than those on T_1W images. Plate dimensions had a significant impact on the absolute extent of artefacts, however increasing thickness, length and width had no influence on the relative amount of susceptibility artefacts. UTE and SEMAC for metal artefact reduction both significantly reduced the extent of artefacts.

Conventional techniques

For the reduction of metal artefacts several techniques are available. For patients with plates and screws adjacent to the bone and with oncological questions, a 1.5 T instead of a 3 T may be used, since decreased magnetic field strength is known to reduce metal artefacts.[15] Also, with increasing artefact level at 3 T, artefact reduction with currently available techniques is limited in several aspects, including the maximum power of the gradient and radiofrequency transmit hardware or patient heating.[15] However, since image resolution is increased in 3 T, the use of metal artefact reduction sequences may be more favourable than changing the respective scanner. Another conventional approach for the sake of improved oncoradiological diagnosis is to use T_1W instead of T_2W sequences, since metal artefacts are being reduced with shorter TEs. Accordingly, in our study, artefacts of all metal plates were more pronounced in T_2W sequences.

UTE and SEMAC

This is also the guiding principle behind UTE sequence with a significant reduction of artefacts for all metallic (TI and MG) systems used in the current study. With UTE, artefact reduction was highest for plates with the largest dimensions and the effect was mostly pronounced for the plates' height, accordingly the diameter that was

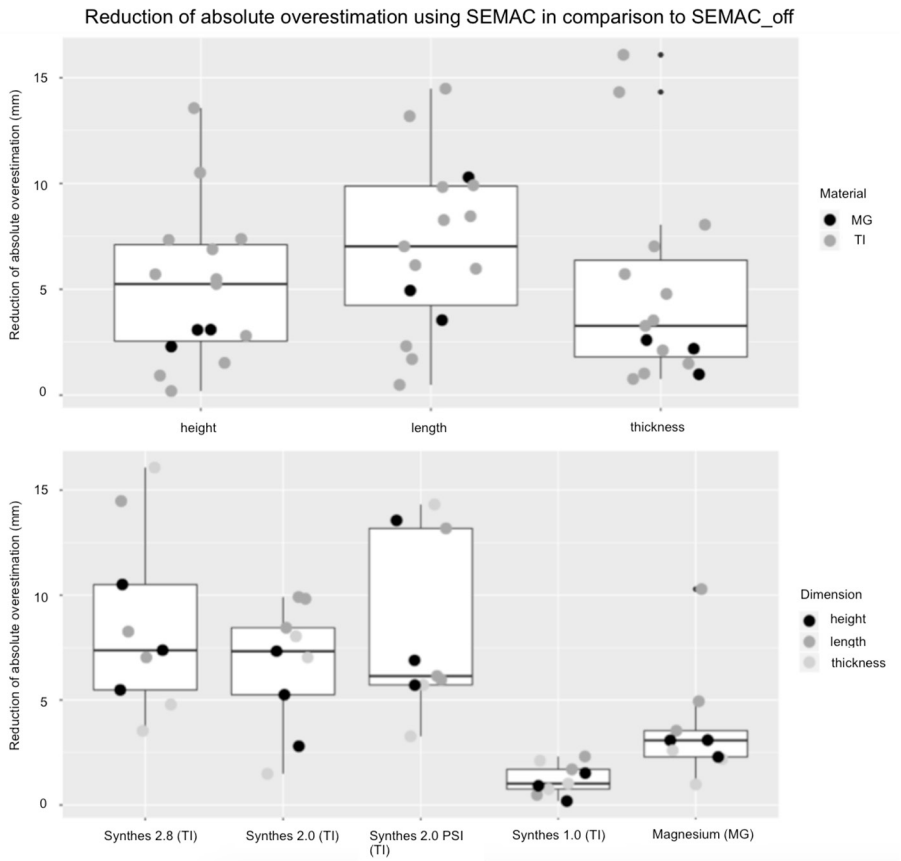

Figure 5 Reduction of absolute artefact overestimation for titanium and magnesium plates using SEMAC in comparison to SEMAC_off. MG, magnesium; SEMAC, slice encoding for metal artefacts; TI, titanium.

placed in the *z*-direction. This is not surprising, since implant positioning is known to be a relevant influence variable for the extent of artefacts and those are expected to be lowest in the longitudinal axis of a metal plate.

SEMAC combines VAT and a reduction of additional through-plane distortions by correcting for signal that is excited in wrong slice positions and is thus superior to standard MR sequences, high bandwidth protocols and simple VAT.[15,28–31] In the current study, the absolute artefact reduction increased with plate dimensions. Interestingly, contrary to UTE, the extent of artefact reduction in different directions was non-uniform.

Regarding the potential usefulness of SEMAC and UTE pulse sequences to reduce TI-induced metal artefacts in MRI, our results are in accordance with previous studies.[28–32] Lu et al[29] demonstrated the efficacy of SEMAC with feasible scan times for the spine and knee region. Reichert et al[30] demonstrated improved image quality in both, tissue specimen and human imaging. While the image quality seems to be superior to conventional and alternative scan protocols including VAT regarding metal artefact production, this method increases scan time, which is disadvantageous in clinical routine.[30] Since a longer period of motionless positioning may be even more problematic to patients with or in condition after diagnosis and surgical treatment of malignoma of the oral cavity including complicated airway management and swallowing during prolonged lying, the clinical feasibility of this protocol in tumour aftercare programs has yet to be demonstrated. Also, for both UTE and SEMAC, future studies will have to proof clinical usefulness regarding diagnostic specificity and sensitivity of primary and recurrent head and neck cancer.

Plate design and material thickness

Regarding the type of system for fixating osseous free flaps at the jaws, to date there is no accepted standard. This may partially be attributable to the lack of valid data regarding clinical, biomechanical and radiological aspects of each system. Compared to the use of 1.0 mm miniplates, thicker plates were recently discussed to potentially increase the rate of soft tissue complications especially in combination with radiotherapy, but no significant difference was found in a comparative analysis.[33] Regarding biomechanical aspects, there are studies promoting miniplates[34] or reconstruction plates.[35] CAD/CAM plates have recently been demonstrated to increase fixation stiffness in comparison to conventional systems,[36] but it is yet unknown, which

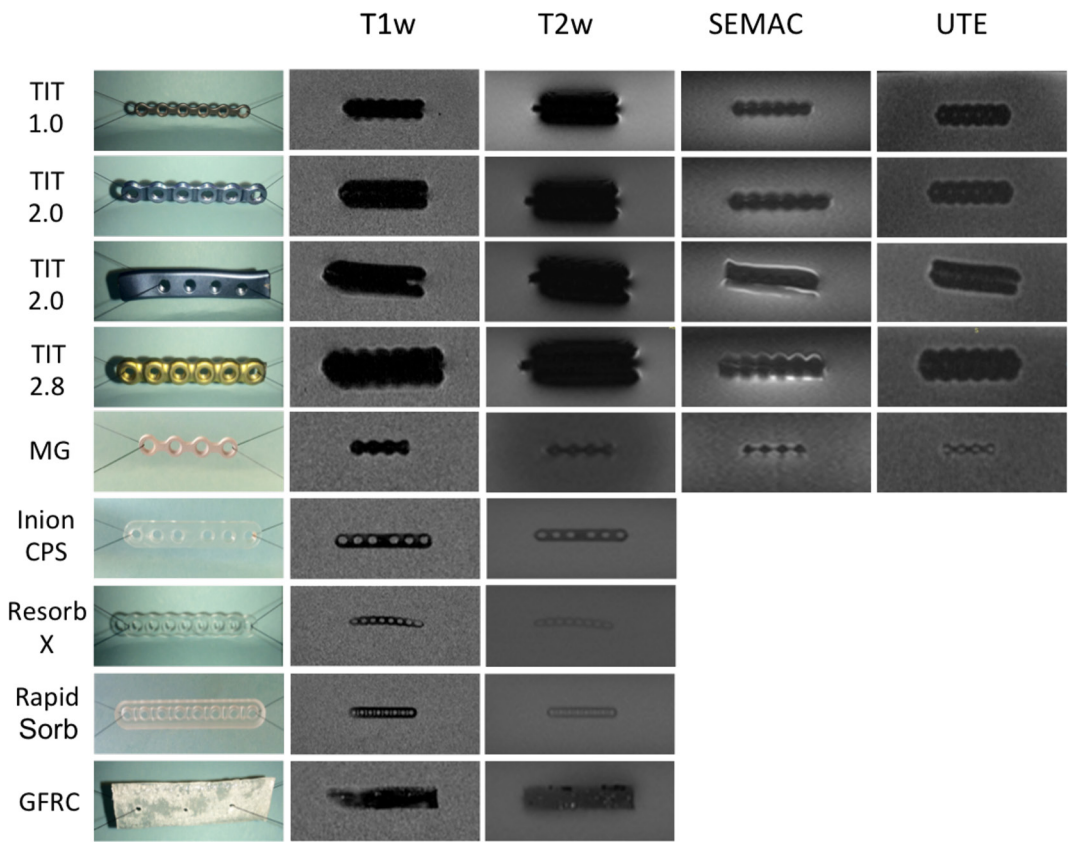

Figure 6 Illustration of all plates and sequences used for each plate. SEMAC, slice encoding for metal artefacts; UTE, ultrashort echo time.

stiffness and thus interosteotomy gap movement range is optimal for bone healing. Implant size and material are relevant parameters for artefact induction and a symmetric and complex shapes and sharp edges in particular are disadvantageous.[15,37,38] In consideration of the results of our study, plates with reduced measures in all dimensions (length, width, thickness) seem more favourable. However, without the combination of plates and screws simulating a realistic fixation type for standard reconstructions, yet no final conclusion can be drawn. For example, a one segment mandible reconstruction with a fibula free flap can be fixed with either 4 miniplates with monocortical screws or one reconstruction bar of varying thickness, height and length with only few or many mono- or bicortical locking or non-locking screws. Alternatively, patient specific plates with asymmetric design and only as many holes as needed for screw fixation and thus increased material consumption can be used. According to the results of our study, more metal is associated with more artefacts and CAD/CAM plates as we know them from several manufacturers, induce significantly more artefacts in MR imaging. Thus, adaptions of design may be necessary in order to increase postoperative imaging quality for the sake of potential recurrent cancer detection.

Biomaterials

In the current study, all tested materials induced significantly less artefacts compared to TI. Despite the fact that it is not possible to draw final conclusions regarding absolute artefact induction when comparing plates of different design and diameters, certain trends become obvious from the results of this study.

Regarding biostable GFRC, patient individual implants made of this material were successfully used for the reconstruction of midfacial defects and cranioplasty.[20,39–42] Recent investigations proved it promising for further clinical applications because of its excellent mechanical properties and osteoconductive potential when used in combination with bioactive glass particulates.[19,26,39,43,44] However, to date, this material has not been used for the fixation of osseous flaps or in trauma cases and therefore, implants and fixed most often with self-drilling TI screws. For the fixation of implants of this kind, there is no screw of the same material provided to date. Accordingly, when considering GFRC for midfacial or even mandible reconstructions in combination with osseous flaps, biomechanical testing with special regards to material interface of plates and screws of varying material, most likely TI, is needed. In this regard, it will be important to analyze potential inflammatory reactions towards composite, glass-fibres and bioactive glass particulates. Recently, GFRC has

been demonstrated to cause only moderate inflammatory reactions in a critical size calvarial bone defect.[45] Whether or not this response may be increased if cyclic dynamic loading causes friction between TI screws and GFRC plates, will have to be critically reflected. GFRC has radiopacity close to that of cortical bone. Higher radiopacity and slightly more visible artefacts of the GFRC compared to polylactide is due to glass fibres in the polymer matrix.

Bioabsorbable plating systems based on synthetic PLLA or PDLLA are known to provide less fatigue strength compared to TI. In this regard, the Inion system, among others, was recently demonstrated to be superior to the products of other manufacturers.[46–48] However, reasonable polymers may be used in situations where loading forces are expected to be low.[16,17] This applies for midfacial reconstructions and, referring to postoperative bite force analyses, may also be attributable to patients after mandible reconstruction.[49,50] Accordingly, a recent investigation on free flap reconstructions demonstrated clinical feasibility.[51] However, biomechanical studies setting resorbable plates under torsion strength should be performed, before clinical application may be recommended. Additionally, the degradation process, which is mainly acidic hydrolysis, may be unfavourable for reconstructive osseous indications, because it has been correlated with impaired bone and wound healing as well as increased foreign body reactions[52,53]

MG has not been extensively used for clinical applications due to its rapid degradation causing hydrogen gas formation and inflammatory response.[24] However, recent investigations with uncoated and modified MG alloys showed promising results with increased cytocompatibility *in vitro* and *in vivo*.[21,54] In contrast to polylactide, MG degradation is alkaline and the byproducts further react with physiological compounds in a bone promoting manner.[52] In comparison to TI, MG plates produce less susceptibility artefacts, which may further encourage studies and developments towards a clinically advisable fixation system. Since SEMAC and UTE reduced metal artefacts also for MG, using metal artefact reduction sequences may help to improve diagnostic image quality in these patients, too.

Limitations

Even although our study was particularly chosen to simulate the clinical setting, a limitation of the present study was its *in vitro* setup. However, distinct positioning of the plates in the scanners mimicking the clinical setting and the application of standard protocols, dedicated for head and neck imaging in patients in the clinical setting were applied to obtain measurements closely reflecting the *in vivo* situation.

Nevertheless, it is only partially possible to simulate a clinical situation, since *in vivo*, the presence of adjacent anatomical structures can influence intensity measurements. Therefore, the intensity and geometric distribution of artefacts in MRI could have been modified by the *in vitro* setup.

Also, the use of plates of different size and diameter is a critical aspect when comparing artefacts in MRI. From a technical and conceptional point of view, the comparison of same size and design plates, *e.g.* all miniplates, could deliver more valid data regarding the extent of absolute artefacts, when the question was to exactly compare the artefact potential of different biomaterials. For a more profound understanding, also TI plates and alloys of different manufacturers could have been included.

Accordingly, further studies are needed to test, whether the differences reported here in artefact induction will hold true after combination of different plating systems with fixation screws inserted into bone. While the generally increased dimensions of locking fixation plates have caused significantly more imaging artefacts in both, T_1W and T_2W sequences compared to miniplates, this might not be the case adjacent to bone. In this regard, also the number and type of fixation screws will have to be evaluated, since (locking) screws for reconstruction plates are usually longer and thicker than screws used in combination with miniplates, but more screws are needed to fix a transplant with miniplates.

Conclusion

In conclusion, the knowledge about the amount and distribution of artefacts induced by different fixation plates of various materials might help to support the decision for choice of implant material in the clinical setting. According to our results, PL, GFRC and MG plates seem to produce less susceptibility artefacts in MRI compared to TI. Furthermore, the dimensions of TI implants directly influence artefact extension. With SEMAC and UTE, metal artefacts can be reduced significantly. Future studies are needed to evaluate artefacts of plates and screws adjacent to bone and soft tissue and to compare different methods of fixation with same size plates.

Acknowledgements

We thank Joachim Graessner from Siemens Healthineers for providing us with SEMAC and UTE sequences for this study and for helping us to revise the manuscript. Special thanks to Ms. Janne Rehberg from the Research Department of Oral and Maxillofacial Surgery, University Medical Center Hamburg Eppendorf for helping to embed the samples.

References

1. Camuzard O, Dassonville O, Ettaiche M, Chamorey E, Poissonnet G, Berguiga R, et al. Primary radical ablative surgery and fibula free-flap reconstruction for T4 oral cavity squamous cell carcinoma with mandibular invasion: oncologic and functional results and their predictive factors. *Eur Arch Otorhinolaryngol* 2017; **274**: 441–9. doi: https://doi.org/10.1007/s00405-016-4219-7
2. Miyamoto Y, Tani T. Reconstruction of mandible with free osteocutaneous flap using deep circumflex iliac vessels as the stem. *Ann Plast Surg* 1981; **6**: 354–61. doi: https://doi.org/10.1097/00000637-198105000-00003
3. Borbély L, Kärcher H. Reconstruction of the maxilla by a microsurgical method and bone transplantation using bone from the scapula. *Fogorv Sz* 1991; **84**: 39–42.
4. Al-Bustani S, Austin GK, Ambrose EC, Miller J, Hackman TG, Halvorson EG. Miniplates versus reconstruction bars for oncologic free fibula flap mandible reconstruction. *Ann Plast Surg* 2016; **77**: 314–7. doi: https://doi.org/10.1097/SAP.0000000000000497
5. Hidalgo DA. Fibula free flap: a new method of mandible reconstruction. *Plast Reconstr Surg* 1989; **84**: 71–9.
6. Rodriguez ED, Bluebond-Langner R, Martin M, Manson PN. Deep circumflex iliac artery free flap in mandible reconstruction. *Atlas Oral Maxillofac Surg Clin North Am* 2006; **14**: 151–9. doi: https://doi.org/10.1016/j.cxom.2006.05.004
7. Rendenbach C, Hölterhoff N, Hischke S, Kreutzer K, Smeets R, Assaf AT, et al. Free flap surgery in Europe: an interdisciplinary survey. *Int J Oral Maxillofac Surg* 2018; **47**: 676-682. doi: https://doi.org/10.1016/j.ijom.2017.11.013
8. Hermans R. Posttreatment imaging in head and neck cancer. *Eur J Radiol* 2008; **66**: 501–11. doi: https://doi.org/10.1016/j.ejrad.2008.01.021
9. Vandecaveye V, De Keyzer F, Nuyts S, Deraedt K, Dirix P, Hamaekers P, et al. Detection of head and neck squamous cell carcinoma with diffusion weighted MRI after (chemo) radiotherapy: correlation between radiologic and histopathologic findings. *Int J Radiat Oncol Biol Phys* 2007; **67**: 960–71. doi: https://doi.org/10.1016/j.ijrobp.2006.09.020
10. Abbaszadeh K, Heffez LB, Mafee MF. Effect of interference of metallic objects on interpretation of T1-weighted magnetic resonance images in the maxillofacial region. *Oral Surg Oral Med Oral Pathol Oral Radiol Endod* 2000; **89**: 759–65. doi: https://doi.org/10.1067/moe.2000.105942
11. Eggers G, Rieker M, Kress B, Fiebach J, Dickhaus H, Hassfeld S. Artefacts in magnetic resonance imaging caused by dental material. *MAGMA* 2005; **18**: 103–11. doi: https://doi.org/10.1007/s10334-005-0101-0
12. Tymofiyeva O, Vaegler S, Rottner K, Boldt J, Hopfgartner AJ, Proff PC, et al. Influence of dental materials on dental MRI. *Dentomaxillofac Radiol* 2013; **42**: 20120271. doi: https://doi.org/10.1259/dmfr.20120271
13. Pompa V, Galasso S, Cassetta M, Pompa G, De Angelis F, Di Carlo S. A comparative study of magnetic resonance (MR) and computed tomography (CT) in the pre-implant evaluation. *Ann Stomatol* 2010; **1**: 33–8.
14. Smeets R, Schöllchen M, Gauer T, Aarabi G, Assaf AT, Rendenbach C, et al. Artefacts in multimodal imaging of titanium, zirconium and binary titanium-zirconium alloy dental implants: an in vitro study. *Dentomaxillofac Radiol* 2017; **46**: 20160267. doi: https://doi.org/10.1259/dmfr.20160267
15. Jungmann PM, Agten CA, Pfirrmann CW, Sutter R. Advances in MRI around metal. *J Magn Reson Imaging* 2017; **46**: 972–91. doi: https://doi.org/10.1002/jmri.25708
16. Suzuki SI Y. *Biomaterialis for surgical operation*. New York, Dordrecht, Heidelberg, London: Springer; 2012.
17. Buijs GJ, van der Houwen EB, Stegenga B, Bos RR, Verkerke GJ. Mechanical strength and stiffness of biodegradable and titanium osteofixation systems. *J Oral Maxillofac Surg* 2007; **65**: 2148–58. doi: https://doi.org/10.1016/j.joms.2007.04.010
18. Peltola MJ, Aitasalo KM, Suonpää JT, Yli-Urpo A, Laippala PJ, Forsback AP. Frontal sinus and skull bone defect obliteration with three synthetic bioactive materials. A comparative study. *J Biomed Mater Res B Appl Biomater* 2003; **66**: 364–72. doi: https://doi.org/10.1002/jbm.b.10023
19. Piitulainen JM. *Reconstruction of cranial bone defects with fiber-reinforced composite-bioactive glass implants*. Turku: University of Turku; 2015.
20. Posti JP, Piitulainen JM, Hupa L, Fagerlund S, Frantzén J, Aitasalo KMJ, et al. A glass fiber-reinforced composite - bioactive glass cranioplasty implant: A case study of an early development stage implant removed due to a late infection. *J Mech Behav Biomed Mater* 2015; **55**: 191–200. doi: https://doi.org/10.1016/j.jmbbm.2015.10.030
21. Chaya A, Yoshizawa S, Verdelis K, Myers N, Costello BJ, Chou DT, et al. In vivo study of magnesium plate and screw degradation and bone fracture healing. *Acta Biomater* 2015; **18**: 262–9. doi: https://doi.org/10.1016/j.actbio.2015.02.010
22. Chaya A, Yoshizawa S, Verdelis K, Noorani S, Costello BJ, Sfeir C. Fracture healing using degradable magnesium fixation plates and screws. *J Oral Maxillofac Surg* 2015; **73**: 295–305. doi: https://doi.org/10.1016/j.joms.2014.09.007
23. Filli L, Luechinger R, Frauenfelder T, Beck S, Guggenberger R, Farshad-Amacker N, et al. Metal-induced artifacts in computed tomography and magnetic resonance imaging: comparison of a biodegradable magnesium alloy versus titanium and stainless steel controls. *Skeletal Radiol* 2015; **44**: 849–56. doi: https://doi.org/10.1007/s00256-014-2057-5
24. Sonnow L, Könneker S, Vogt PM, Wacker F, von Falck C. Biodegradable magnesium Herbert screw - image quality and artifacts with radiography, CT and MRI. *BMC Med Imaging* 2017; **17**: 16. doi: https://doi.org/10.1186/s12880-017-0187-7
25. Kuusisto N, Vallittu PK, Lassila LV, Huumonen S. Evaluation of intensity of artefacts in CBCT by radio-opacity of composite simulation models of implants in vitro. *Dentomaxillofac Radiol* 2015; **44**: 20140157. doi: https://doi.org/10.1259/dmfr.20140157
26. Vallittu PK. The effect of glass fiber reinforcement on the fracture resistance of a provisional fixed partial denture. *J Prosthet Dent* 1998; **79**: 125–30. doi: https://doi.org/10.1016/S0022-3913(98)70204-5
27. Agarwal M, Koelling KW, Chalmers JJ. Characterization of the degradation of polylactic acid polymer in a solid substrate environment. *Biotechnol Prog* 1998; **14**: 517–26. doi: https://doi.org/10.1021/bp980015p
28. Lu W, Pauly KB, Gold GE, Pauly JM, Hargreaves BA. Slice encoding for metal artifact correction with noise reduction. *Magn Reson Med* 2011; **65**: 1352–7. doi: https://doi.org/10.1002/mrm.22796
29. Lu W, Pauly KB, Gold GE, Pauly JM, Hargreaves BA. SEMAC: slice encoding for metal artifact correction in MRI. *Magn Reson Med* 2009; **62**: 66–76. doi: https://doi.org/10.1002/mrm.21967
30. Reichert M, Ai T, Morelli JN, Nittka M, Attenberger U, Runge VM. Metal artefact reduction in MRI at both 1.5 and 3.0 T using slice encoding for metal artefact correction and view angle tilting. *Br J Radiol* 2015; **88**: 20140601. doi: https://doi.org/10.1259/bjr.20140601
31. Hargreaves BA, Chen W, Lu W, Alley MT, Gold GE, Brau AC, et al. Accelerated slice encoding for metal artifact correction. *J Magn Reson Imaging* 2010; **31**: 987–96. doi: https://doi.org/10.1002/jmri.22112
32. Cortes AR, Abdala-Junior R, Weber M, Arita ES, Ackerman JL. Influence of pulse sequence parameters at 1.5 T and 3.0 T on MRI artefacts produced by metal-ceramic restorations. *Dentomaxillofac Radiol* 2015; **44**: 20150136. doi: https://doi.org/10.1259/dmfr.20150136
33. Robey AB, Spann ML, McAuliff TM, Meza JL, Hollins RR, Johnson PJ. Comparison of miniplates and reconstruction plates in fibular flap reconstruction of the mandible. *Plast Reconstr Surg* 2008; **122**: 1733–8.
34. Grohmann I, Raith S, Kesting M, Rau A, Mücke T, Lethaus B, et al. Experimental biomechanical study of the primary stability

of different osteosynthesis systems for mandibular reconstruction with an iliac crest graft. *Br J Oral Maxillofac Surg* 2013; **51**: 942–7. doi: https://doi.org/10.1016/j.bjoms.2013.07.004
35. Fontana SC, Smith RB, Nazir N, Andrews BT. Biomechanical assessment of fixation methods for segmental mandible reconstruction with fibula in the polyurethane model. *Microsurgery* 2016; **36**: 330–3. doi: https://doi.org/10.1002/micr.30052
36. Rendenbach C, Sellenschloh K, Gerbig L, Morlock MM, Beck-Broichsitter B, Smeets R, et al. CAD-CAM plates versus conventional fixation plates for primary mandibular reconstruction: a biomechanical in vitro analysis. *J Craniomaxillofac Surg* 2017; **45**: 1878–83.
37. Gupta A, Subhas N, Primak AN, Nittka M, Liu K. Metal artifact reduction: standard and advanced magnetic resonance and computed tomography techniques. *Radiol Clin North Am* 2015; **53**: 531–47. doi: https://doi.org/10.1016/j.rcl.2014.12.005
38. Hargreaves BA, Worters PW, Pauly KB, Pauly JM, Koch KM, Gold GE. Metal-induced artifacts in MRI. *AJR Am J Roentgenol* 2011; **197**: 547–55. doi: https://doi.org/10.2214/AJR.11.7364
39. Aitasalo KM, Piitulainen JM, Rekola J, Vallittu PK. Craniofacial bone reconstruction with bioactive fiber-reinforced composite implant. *Head Neck* 2014; **36**: 722–8. doi: https://doi.org/10.1002/hed.23370
40. Kurunmäki H, Kantola R, Hatamleh MM, Watts DC, Vallittu PK. A fiber-reinforced composite prosthesis restoring a lateral midfacial defect: a clinical report. *J Prosthet Dent* 2008; **100**: 348–52. doi: https://doi.org/10.1016/S0022-3913(08)60235-8
41. Piitulainen JM, Posti JP, Aitasalo KM, Vuorinen V, Vallittu PK, Serlo W. Paediatric cranial defect reconstruction using bioactive fibre-reinforced composite implant: early outcomes. *Acta Neurochir* 2015; **157**: 681–7. doi: https://doi.org/10.1007/s00701-015-2363-2
42. Al -Dam ARC, Riecke B, Gröbe A, Smeets R, Heiland M, Hanken H. Komplexe Rekonstruktion eines kombinierten Schädeldach- und Mittelgesichtsdefekts mit Implantation eines bioaktiven langglasfaserverstärkten Komposits. 65th Conference of the German Society for Oral and Maxillofacial Surgery; June 10th-13th, 2015; Stuttgart. 2015.
43. Erbe EM, Marx JG, Clineff TD, Bellincampi LD. Potential of an ultraporous beta-tricalcium phosphate synthetic cancellous bone void filler and bone marrow aspirate composite graft. *Eur Spine J* 2001; **10**(Suppl 2): S141–6. doi: https://doi.org/10.1007/s005860100287
44. Peltola MJ, Vallittu PK, Vuorinen V, Aho AA, Puntala A, Aitasalo KM. Novel composite implant in craniofacial bone reconstruction. *Eur Arch Otorhinolaryngol* 2012; **269**: 623–8. doi: https://doi.org/10.1007/s00405-011-1607-x
45. Tuusa SM, Peltola MJ, Tirri T, Puska MA, Röyttä M, Aho H, et al. Reconstruction of critical size calvarial bone defects in rabbits with glass-fiber-reinforced composite with bioactive glass granule coating. *J Biomed Mater Res B Appl Biomater* 2008; **84**: 510–9. doi: https://doi.org/10.1002/jbm.b.30898
46. Ricalde P, Caccamese J, Norby C, Posnick JC, Hartman MJ, von Fraunhofer JA. Strength analysis of 6 resorbable implant systems: does heating affect the stress-strain curve? *J Oral Maxillofac Surg* 2008; **66**: 2493–7. doi: https://doi.org/10.1016/j.joms.2008.06.096
47. Ricalde P, Engroff SL, Von Fraunhofer JA, Posnick JC. Strength analysis of titanium and resorbable internal fixation in a mandibulotomy model. *J Oral Maxillofac Surg* 2005; **63**: 1180–3. doi: https://doi.org/10.1016/j.joms.2005.04.019
48. Buijs GJ, van der Houwen EB, Stegenga B, Bos RR, Verkerke GJ. Mechanical strength and stiffness of biodegradable and titanium osteofixation systems. *J Oral Maxillofac Surg* 2007; **65**: 2148–58. doi: https://doi.org/10.1016/j.joms.2007.04.010
49. Curtis DA, Plesh O, Miller AJ, Curtis TA, Sharma A, Schweitzer R, et al. A comparison of masticatory function in patients with or without reconstruction of the mandible. *Head Neck* 1997; **19**: 287–96. doi: https://doi.org/10.1002/(SICI)1097-0347(199707)19:4<287::AID-HED7>3.0.CO;2-X
50. Maurer P, Pistner H, Schubert J. Computer assisted chewing power in patients with segmental resection of the mandible. *Mund Kiefer Gesichtschir* 2006; **10**: 37–41. doi: https://doi.org/10.1007/s10006-005-0656-y
51. Kim NK, Nam W, Kim HJ. Comparison of miniplates and biodegradable plates in reconstruction of the mandible with a fibular free flap. *Br J Oral Maxillofac Surg* 2015; **53**: 223–9. doi: https://doi.org/10.1016/j.bjoms.2014.11.010
52. Naujokat H, Seitz JM, Açil Y, Damm T, Möller I, Gülses A, et al. Osteosynthesis of a cranio-osteoplasty with a biodegradable magnesium plate system in miniature pigs. *Acta Biomater* 2017; **62**: 434–45. doi: https://doi.org/10.1016/j.actbio.2017.08.031
53. Bergsma EJ, Rozema FR, Bos RR, de Bruijn WC. Foreign body reactions to resorbable poly(L-lactide) bone plates and screws used for the fixation of unstable zygomatic fractures. *J Oral Maxillofac Surg* 1993; **51**: 666–70. doi: https://doi.org/10.1016/S0278-2391(10)80267-8
54. Jung O, Smeets R, Porchetta D, Kopp A, Ptock C, Müller U, et al. Optimized in vitro procedure for assessing the cytocompatibility of magnesium-based biomaterials. *Acta Biomater* 2015; **23**: 354–63. doi: https://doi.org/10.1016/j.actbio.2015.06.005